




New effective interactions for hypernuclei in a density-dependent relativistic mean field model

Yu-Ting Rong (荣宇婷) ^{1,2}, Zhong-Hao Tu (涂中豪) ^{1,2} and Shan-Gui Zhou (周善贵) ^{1,2,3,4,*}

¹CAS Key Laboratory of Theoretical Physics, Institute of Theoretical Physics, Chinese Academy of Sciences, Beijing, 100190, China

²School of Physical Sciences, University of Chinese Academy of Sciences, Beijing, 100049, China

³Center of Theoretical Nuclear Physics, National Laboratory of Heavy Ion Accelerator, Lanzhou, 730000, China

⁴Synergetic Innovation Center for Quantum Effects and Application, Hunan Normal University, Changsha, 410081, China



(Received 4 August 2021; revised 8 October 2021; accepted 15 November 2021; published 29 November 2021)

New effective ΛN interactions are proposed for the density-dependent relativistic mean-field model. The multidimensionally constrained relativistic mean-field model is used to calculate ground-state properties of eleven known Λ hypernuclei with $A \geq 12$ and the corresponding core nuclei. Based on effective NN interactions DD-ME2 and PKDD, the ratios R_σ and R_ω of scalar and vector coupling constants between ΛN and NN interactions are determined by fitting calculated Λ separation energies to experimental values. We propose six new effective interactions for Λ hypernuclei: DD-ME2-Y1, DD-ME2-Y2, DD-ME2-Y3, PKDD-Y1, PKDD-Y2, and PKDD-Y3 with three ways of grouping and including these eleven hypernuclei in the fitting. It is found that the two ratios R_σ and R_ω correlate well and a good linear relation exists between them. The statistical errors of the ratio parameters in these effective interactions are analyzed. These new effective interactions are used to study the single- Λ excited states, the equation of state of hypernuclear matter, and neutron-star properties with hyperons.

DOI: [10.1103/PhysRevC.104.054321](https://doi.org/10.1103/PhysRevC.104.054321)

I. INTRODUCTION

Hyperon-nucleon (YN) interaction is an important part of baryon-baryon interactions [1–6]. It is crucial for understanding the structure of hypernuclei and the properties of compact stars and vice versa, i.e., the studies of hypernuclear structure and compact stars are crucial for constraining the YN interaction [7,8]. Many experiments have been carried out to study hypernuclear structure at the Large Hadron Collider (LHC), the Double Annular Φ Factory for Nice Experiments (DAΦNE), the Jefferson Laboratory (JLab), the Japan Proton Accelerator Research Complex (J-PARC), the Mainz Microtron (MAMI), the Relativistic Heavy Ion Collider (RHIC), and the GSI Helmholtz Centre for Heavy Ion Research (GSI) [9–14]. The investigations of single Λ , double Λ [15], Ξ hypernuclei [16,17], and antihypernuclei [18] have provided valuable information on YN and YY interactions. From the theory side, the SU(3) flavor symmetry, which reveals the relation between baryon and meson octet states, is generally used for determining the YN interaction. With the constraint of SU(3) flavor symmetry or experimental observables, many approaches, such as lattice QCD [19–22], the chiral effective-field theory [23–25], the Nijmegen soft-core model [2,26,27], the Jülich hyperon-nucleon model [28–30], the Skyrme Hartree-Fock model [31–33], and the relativistic mean-field (RMF) model [34–37], have been used to study the structure of hypernuclei based on various (effective) YN and YY interactions.

In the RMF model proposed by Walecka [38], there are only linear coupling terms in the interaction Lagrangian, i.e., mesons do not interact between themselves. Such linear couplings lead to an improper description of the incompressibility of nuclear matter and surface properties in finite nuclei. To describe adequately these essential nuclear properties, either nonlinear (NL) self-couplings of meson fields [39–43] or density-dependent (DD) nucleon-meson couplings [44–50] have been introduced in the RMF model. The NL-RMF model has been extended and widely applied to the study of hypernuclei and many effective interactions have been proposed. However, there are much fewer DD-RMF effective interactions for hypernuclei [51–58]. The effective ΛN interactions were usually obtained by fitting the calculated Λ separation energies to experimental values of known hypernuclei and, in the fitting procedure, the RMF calculations were carried out with the restriction of spherical symmetry. Yet most observed hypernuclei are deformed and there are only a few spherical hypernuclei. In this paper, we propose new DD effective interactions for hypernuclei by using a deformed RMF model—the multidimensionally constrained (MDC) RMF model.

The paper is organized as follows: In Sec. II, we introduce the MDC-RMF model for Λ hypernuclei with density-dependent couplings. In Sec. III, we present our results and discuss Λ separation energies, deformation effects, parameter correlations, and neutron-star properties with the new effective interactions. Finally, a summary is given in Sec. IV.

II. THEORETICAL FRAMEWORK

The RMF model has been very successful in describing properties of nuclear matter and finite nuclei in the whole

*sgzhou@itp.ac.cn

nuclear chart [59–69]. Both the NL-RMF and DD-RMF models have been extended to the study of hypernuclei

[34–37,51–58,70–79]. In the DD-RMF model, the Lagrangian for a Λ hypernucleus is written as

$$\begin{aligned} \mathcal{L} = & \sum_B \bar{\psi}_B \left(i\gamma_\mu \partial^\mu - M_B - g_{\sigma B} \sigma - g_{\sigma^* B} \sigma^* - g_{\omega B} \gamma_\mu \omega^\mu - g_{\phi B} \gamma_\mu \phi^\mu - g_{\rho B} \gamma_\mu \vec{\tau} \cdot \vec{\rho}^\mu - e\gamma_\mu \frac{1-\tau_3}{2} A^\mu \right) \psi_B \\ & + \psi_\Lambda \frac{f_{\omega\Lambda\Lambda}}{4M_\Lambda} \sigma_{\mu\nu} \Omega^{\mu\nu} \psi_\Lambda + \frac{1}{2} \partial^\mu \sigma \partial_\mu \sigma - \frac{1}{2} m_\sigma^2 \sigma^2 + \frac{1}{2} \partial_\mu \sigma^* \partial^\mu \sigma^* - \frac{1}{2} m_{\sigma^*}^2 \sigma^{*2} - \frac{1}{4} \Omega^{\mu\nu} \Omega_{\mu\nu} + \frac{1}{2} m_\omega^2 \omega^\mu \omega_\mu \\ & - \frac{1}{4} S^{\mu\nu} S_{\mu\nu} + \frac{1}{2} m_\phi^2 \phi^\mu \phi_\mu - \frac{1}{4} \vec{R}^{\mu\nu} \vec{R}_{\mu\nu} + \frac{1}{2} m_\rho^2 \vec{\rho}^\mu \vec{\rho}_\mu - \frac{1}{4} F^{\mu\nu} F_{\mu\nu}, \end{aligned} \quad (1)$$

where B represents neutron, proton, or Λ , and M_B is the corresponding mass. σ and σ^* are scalar-isoscalar meson fields coupled to baryons, ω^μ and ϕ^μ are vector-isoscalar meson fields coupled to baryons, $\vec{\rho}^\mu$ is the vector-isovector meson field coupled to nucleons, and A^μ is the photon field. $\Omega_{\mu\nu}$, $S_{\mu\nu}$, $\vec{R}_{\mu\nu}$, and $F_{\mu\nu}$ are field tensors of the vector mesons ω^μ , ϕ^μ , $\vec{\rho}^\mu$, and photons A^μ . m_σ ($g_{\sigma B}$), m_{σ^*} ($g_{\sigma^* B}$), m_ω ($g_{\omega B}$), m_ϕ ($g_{\phi B}$), and m_ρ ($g_{\rho B}$) are the masses (coupling constants) for meson fields. The coupling constants are dependent on the total baryonic density ρ^v ,

$$g_{mB}(\rho^v) = g_{mB}(\rho_{\text{sat}}) f_{mB}(x), \quad x = \rho^v / \rho_{\text{sat}}, \quad (2)$$

where m represents mesons and ρ_{sat} is the saturation density of nuclear matter. $g_{mB}(\rho_{\text{sat}})$, the coupling constant at saturation density, and $f_{mB}(x)$ describing the density dependence are discussed in Sec. III.

Starting from the Lagrangian (1), the equations of motion can be derived via the variational principle. The Dirac equation for baryons reads

$$[\boldsymbol{\alpha} \cdot \mathbf{p} + V_B + T_B + \Sigma_R + \beta(M_B + S_B)]\psi_{iB} = \varepsilon_i \psi_{iB}, \quad (3)$$

the Klein-Gordon equations for mesons and the Proca equation for photon are

$$\begin{aligned} (-\Delta + m_\sigma^2)\sigma &= -g_{\sigma N} \rho_N^s - g_{\sigma\Lambda} \rho_\Lambda^s, \\ (-\Delta + m_{\sigma^*}^2)\sigma^* &= -g_{\sigma^* \Lambda} \rho_\Lambda^s, \\ (-\Delta + m_\omega^2)\omega_0 &= g_{\omega N} \rho_N^v + g_{\omega\Lambda} \rho_\Lambda^v - \frac{f_{\omega\Lambda\Lambda}}{2M_\Lambda} \rho_\Lambda^T, \\ (-\Delta\phi + m_\phi^2)\phi &= g_{\phi\Lambda} \rho_\Lambda^v, \\ (-\Delta + m_\rho^2)\rho_0 &= g_{\rho N} (\rho_n^v - \rho_p^v), \\ -\Delta A_0 &= e\rho_p^v. \end{aligned} \quad (4)$$

Equations (3) and (4) are coupled via the scalar, vector, and tensor densities,

$$\begin{aligned} \rho_B^s &= \sum_i \bar{\psi}_{iB} \psi_{iB}, \\ \rho_B^v &= \sum_i \bar{\psi}_{iB} \boldsymbol{\gamma}^0 \psi_{iB}, \\ \rho_\Lambda^T &= i\partial \left(\sum_i \psi_{i\Lambda}^\dagger \boldsymbol{\gamma} \psi_{i\Lambda} \right), \end{aligned} \quad (5)$$

and various potentials:

$$\begin{aligned} V_B &= g_{\omega B} \omega_0 + g_{\phi B} \phi_0 + g_{\rho B} \tau_3 \rho_0 + e \frac{1-\tau_3}{2} A_0, \\ S_B &= g_{\sigma B} \sigma + g_{\sigma^* B} \sigma^*, \\ T_\Lambda &= -\frac{f_{\omega\Lambda\Lambda}}{2M_\Lambda} \boldsymbol{\beta}(\boldsymbol{\alpha} \cdot \mathbf{p}) \omega_0, \\ \Sigma_R &= \frac{\partial g_{\sigma N}}{\partial \rho^v} \rho_N^s \sigma + \frac{\partial g_{\omega N}}{\partial \rho^v} \rho_N^v \omega_0 + \frac{\partial g_{\rho N}}{\partial \rho^v} (\rho_n^v - \rho_p^v) \rho_0 \\ &+ \frac{\partial g_{\sigma^* \Lambda}}{\partial \rho^v} \rho_\Lambda^s \sigma^* + \frac{\partial g_{\phi \Lambda}}{\partial \rho^v} \rho_\Lambda^v \phi_0 \\ &+ \frac{1}{2M_\Lambda} \frac{\partial f_{\omega\Lambda\Lambda}}{\partial \rho^v} \rho_\Lambda^T \omega_0. \end{aligned} \quad (6)$$

The rearrangement term Σ_R is present in the DD-RMF model to ensure energy-momentum conservation and thermodynamic consistency [48].

Under the mean-field and no-sea approximations, the Dirac equation (3), the Klein-Gordon equations, and the Proca equation (4) have been solved in different bases, including coordinate space [80–83], the harmonic-oscillator basis [84–86], the Woods-Saxon basis [87], and the Lagrange mesh [88]. To simplify the solving procedure of these equations, most RMF models were developed with certain spatial symmetries imposed on nuclei. Note that the solution of the Dirac equation in a three dimensional (3D) lattice was achieved recently and in such a RMF model, the nuclei in question are not restricted by any spatial symmetry [89,90]. In the present work, we use the MDC-RMF model [68,91,92] in which an axially deformed harmonic-oscillator (ADHO) basis [84] is used, the pairing correlations are treated by the BCS approach, and the V_4 symmetry is assumed for nuclear shapes, i.e., all deformations characterized by $\beta_{\lambda\mu}$ with even μ , e.g., β_{20} , β_{22} , β_{30} , β_{32} , β_{40} , . . . , are included self-consistently. The MDC-RMF model has been used to study the potential-energy surfaces and fission barriers of heavy and superheavy nuclei [91–95], nonaxial octupole Y_{32} correlations [96,97], the octupole correlations in chiral doublet bands [98,99], etc.

Both NL and DD couplings have been implemented in the MDC-RMF model for normal nuclei. The MDC-RMF model with NL self-couplings of meson fields has been also extended to Λ hypernuclei [37,75,77]. In the present work, we have included the DD couplings in the MDC-RMF model for Λ hypernuclei and, under the V_4 symmetry, solved Eqs. (3) and

(4) in the ADHO basis. To keep the time-reversal symmetry, when dealing with the unpaired baryon, we adopt the equal filling approximation, which has been widely used in mean-field calculations [100]. The spurious motion due to the breaking of the translational invariance is treated by including the center-of-mass correction $E_{c.m.} = -\langle P^2 \rangle / 2M$ with $M = (A - 1)M_N + M_\Lambda$ in the binding energy.

III. RESULTS AND DISCUSSIONS

In this section we determine the parameters of the coupling constants $g_{mB}(\rho^\nu)$ in Eq. (2) for hypernuclei based on available DD-RMF effective interactions for normal nuclei. For the mesons in Eq. (1), one usually considers σ , ω , and ρ for normal nuclei. In this work, we focus on single- Λ hypernuclei in which σ^* and ϕ can be omitted because they only couple to strange quarks according to the Okub-Zweig-Iizuba (OZI) rule. Furthermore, the electromagnetic field and ρ mesons do not couple to Λ because the Λ hyperon is charge neutral with isospin $\tau = 0$. Therefore, we are left with $g_{\sigma\Lambda}$ and $g_{\omega\Lambda}$ to be fixed. Many DD-RMF effective interactions have been proposed for normal nuclei, e.g., TW99 [49], DD-ME1 [50], PKDD [43], DD-ME2 [101], DD [102], D³C [102], PKO1 and PKO2 [103], PKO3 [104], PKA1 [105], DD2 [106], DDME δ [107], DDME-X [108], DD-LZ1 [109], and DDV, DDS, DDVT, DDST, DDVTD, and DDSTD [110]. Most of them can provide a good description for the properties not only of nuclear matter but also of finite nuclei around and far from the valley of β stability. In this work we choose two typical ones, PKDD [43] and DD-ME2 [101], in which the density dependence in Eq. (2) is taken as

$$f_{mN}(x) = \begin{cases} a_m \frac{1 + b_m(x + d_m)^2}{1 + c_m(x + d_m)^2}, & m = \sigma \text{ or } \omega \\ e^{-a_\rho(x - 1)}, & m = \rho, \end{cases} \quad (7)$$

with nine parameters. Under five constraints, $f_\sigma(1) = 1$, $f_\omega(1) = 1$, $f''_\sigma(0) = 0$, $f''_\omega(0) = 0$, and $f''_\sigma(1) = f''_\omega(1)$, there are four free parameters which have been adjusted to properties of nuclear matter and selected finite nuclei [43,101]. We assume the same density dependence of $g_{m\Lambda}(\rho^\nu)$ as that of $g_{mN}(\rho^\nu)$ ($m = \sigma$ or ω). So there are two parameters $g_{\sigma\Lambda}(\rho_{\text{sat}})$ and $g_{\omega\Lambda}(\rho_{\text{sat}})$ to be determined.

In Λ hypernuclei, the single-particle potential depth for Λ is about 30 MeV [111,112] and the energy splitting between spin partners in single- Λ states is very small compared with that for nucleons [113–115]. The shallow potential and small spin-orbit splittings for Λ have been understood under the following mechanisms: (i) the effective scalar and vector boson exchange interactions with Σ and Δ -isobar intermediate states [116]; (ii) the combined quark-gluon exchange between the valence baryon and the nucleons of the core [117]; (iii) a weak SU(3) symmetry breaking and a tensor $\omega\Lambda\Lambda$ coupling [118,119]. In the RMF model, the last mechanism has been used mostly for the study of Λ hypernuclei [72,75,78,79,120,121]. According to the OZI rule, the tensor coupling constant $f_{\omega\Lambda\Lambda}$ is the same as that of $g_{\omega\Lambda}$ and $R_{\omega\Lambda\Lambda} = f_{\omega\Lambda\Lambda}/g_{\omega\Lambda} = -1.0$ [119,122]. In the present work we follow this convention concerning the tensor coupling between ω

and Λ and assume $f_{\omega\Lambda\Lambda}(\rho^\nu) = -g_{\omega\Lambda}(\rho^\nu)$. According to the quark model, the ratio $R_m = g_{m\Lambda}(\rho_{\text{sat}})/g_{mN}(\rho_{\text{sat}}) = 2/3$ with $m = \sigma$ or ω [34,123,124]. These two ratios, together with the parameters of DD-ME2 or PKDD, define completely the DD-RMF functionals for Λ hypernuclei. We use DD-ME2-Y0 and PKDD-Y0 to label these two effective interactions. Since they cannot give even a decent description for Λ separation energies of hypernuclei with $A \geq 12$, as seen in Table I, we adjust the ratios R_σ and R_ω to the experimental values of Λ separation energies of selected hypernuclei.

To date, Λ separation energies of 33 single- Λ hypernuclei have been measured. Most of these hypernuclei are very light and there are fifteen with $A \geq 12$: $^{12}_\Lambda\text{B}$, $^{12-14}_\Lambda\text{C}$, $^{15,16}_\Lambda\text{N}$, $^{16}_\Lambda\text{O}$, $^{28}_\Lambda\text{Si}$, $^{32}_\Lambda\text{S}$, $^{40}_\Lambda\text{Ca}$, $^{51,52}_\Lambda\text{V}$, $^{89}_\Lambda\text{Y}$, $^{139}_\Lambda\text{La}$, and $^{208}_\Lambda\text{Pb}$. In the present work, the difference of Λ separation energies of mirror hypernuclei, ($^{12}_\Lambda\text{B}$, $^{12}_\Lambda\text{C}$) and ($^{16}_\Lambda\text{N}$, $^{16}_\Lambda\text{O}$), cannot be reproduced because Λ interacts with both protons and neutrons via the exchange of the same mesons and the charge symmetry breaking is not enough. Therefore we select only one hypernucleus in each pair, namely, $^{12}_\Lambda\text{C}$ and $^{16}_\Lambda\text{O}$. $^{14}_\Lambda\text{C}$ and $^{15}_\Lambda\text{N}$ are not included because their separation energies were measured only by using the photographic emulsion technique which should not be trusted for hypernuclei with $A \geq 12$ [7]. To date, all effective YN interactions used in the RMF model were obtained with the restriction of spherical symmetry, although many of the observed hypernuclei are deformed. In this work, we use the MDC-RMF model and consider axial and reflection symmetric deformations when adjusting the parameters of DD-RMF effective interactions. For simplicity, the pairing correlations are ignored.

We first calculate the ground-state properties of the core nuclei of these eleven selected hypernuclei: $^{11,12}_\Lambda\text{C}$, $^{15}_\Lambda\text{O}$, $^{27}_\Lambda\text{Si}$, $^{31}_\Lambda\text{S}$, $^{39}_\Lambda\text{Ca}$, $^{50,51}_\Lambda\text{V}$, $^{88}_\Lambda\text{Y}$, $^{138}_\Lambda\text{La}$, and $^{207}_\Lambda\text{Pb}$. The relative deviations of the calculated binding energies from the experimental values are shown in Fig. 1(a). The experimental binding energies are taken from AME2016 [125]. From Fig. 1(a), one can see that binding energies calculated with both DD-ME2 and PKDD are close to the experimental values for all of these nuclei. The relative deviations from AME2016 are within 5% and the largest deviation occurs for $^{12}_\Lambda\text{C}$. Except $^{15}_\Lambda\text{O}$ and $^{207}_\Lambda\text{Pb}$, all other nuclei are deformed, although $^{39}_\Lambda\text{Ca}$ is almost spherical, as seen in Fig. 1(b). From MDC-RMF calculations with PKDD and DD-ME2, similar deformations are obtained for ten of these eleven nuclei with $^{11}_\Lambda\text{C}$ as an exception: $^{11}_\Lambda\text{C}$ is oblate with DD-ME2 but prolate with PKDD.

Based on effective NN interactions DD-ME2 and PKDD, the mass of the Λ hyperon is fixed at 1115.6 MeV and the two ratios R_σ and R_ω are determined by minimizing the average square deviation,

$$\bar{\chi}^2(\mathbf{a}) = \frac{1}{N} \sum_i \left(\frac{B_{\Lambda,i}^{\text{expt.}} - B_{\Lambda,i}^{\text{calc.}}(x_i; \mathbf{a})}{\Delta B_{\Lambda,i}^{\text{expt.}}} \right)^2, \quad (8)$$

where \mathbf{a} is the ensemble of parameters to be determined (R_σ and R_ω), i numbers each hypernucleus, B_Λ is the separation energy, and $\Delta B_{\Lambda,i}^{\text{expt.}}$ represents the experimental uncertainty. The experimental values of $B_{\Lambda,i}^{\text{expt.}}$ and $\Delta B_{\Lambda,i}^{\text{expt.}}$ are taken from Ref. [7] and references therein, except for $^{40}_\Lambda\text{Ca}$ for which

TABLE I. The calculated Λ separation energies B_Λ (in MeV) for selected hypernuclei with DD-ME2- Yi and PKDD- Yi ($i = 0, 1, 2$, and 3) in comparison with experimental values. $\bar{\chi}^2$ ($\bar{\chi}_{\text{all}}^2$) represents the average least-square deviation of the calculated Λ separation energies of hypernuclei in each group (all eleven hypernuclei) from the experimental values. The bold-faced B_Λ values denote that the experimental values of the corresponding hypernuclei are used in the parametrization fitting. See text for the grouping of hypernuclei used in the fitting. The root mean square (rms) deviation Δ is given in MeV and the root of relative square (rrs) deviation δ is in percent. The corresponding ratios R_σ and R_ω of the effective ΛN interactions together with statistical errors $\sigma_{R_\sigma}^+$ and $\sigma_{R_\sigma}^-$ of R_σ are listed at the bottom of the table. The tensor coupling constant $f_{\omega\Lambda\Lambda} = -g_{\omega\Lambda}$.

Hypernucleus	Expt.	DD-ME- Yi				PKDD- Yi			
		$i = 0$	$i = 1$	$i = 2$	$i = 3$	$i = 0$	$i = 1$	$i = 2$	$i = 3$
$^{12}_\Lambda\text{C}$	11.36 ± 0.20	25.514	10.789	10.588	10.120	25.566	10.854	10.514	10.013
$^{13}_\Lambda\text{C}$	12.0 ± 0.2	28.080	12.262	12.023	11.422	27.814	11.932	11.534	10.944
$^{16}_\Lambda\text{O}$	13.0 ± 0.2	27.516	12.849	12.643	12.174	27.771	13.089	12.684	12.105
$^{28}_\Lambda\text{Si}$	17.2 ± 0.2	34.724	17.643	17.560	17.450	34.857	17.731	17.578	17.469
$^{32}_\Lambda\text{S}$	17.5 ± 0.5	36.814	18.865	18.895	18.827	36.341	18.824	18.695	18.640
$^{40}_\Lambda\text{Ca}$	18.7 ± 1.1	36.600	19.566	19.448	19.265	36.730	19.756	19.493	19.235
$^{51}_\Lambda\text{V}$	21.5 ± 0.6	39.126	21.227	21.228	21.401	39.095	21.251	21.221	21.407
$^{52}_\Lambda\text{V}$	21.8 ± 0.3	39.429	21.422	21.440	21.662	39.348	21.400	21.402	21.649
$^{89}_\Lambda\text{Y}$	23.6 ± 0.5	41.882	23.511	23.576	23.974	41.788	23.501	23.578	24.018
$^{139}_\Lambda\text{La}$	25.1 ± 1.2	42.691	24.306	24.479	25.215	42.226	23.987	24.295	25.210
$^{208}_\Lambda\text{Pb}$	26.9 ± 0.8	44.489	25.687	25.893	26.746	44.029	25.337	25.694	26.729
$\bar{\chi}^2$			2.543	1.867	0.185		2.580	1.889	0.211
$\bar{\chi}_{\text{all}}^2$		2956.907	2.543	3.009	6.690	2954.595	2.580	3.666	9.233
Δ		17.175	0.711	0.672	0.668	17.048	0.816	0.712	0.716
δ		98.221	3.759	3.840	4.817	97.776	4.018	4.060	5.419
R_σ		0.667	0.366	0.417	0.577	0.667	0.367	0.464	0.659
R_ω		0.667	0.352	0.415	0.611	0.667	0.353	0.472	0.712
$\sigma_{R_\sigma}^+$			0.053	0.036	0.080		0.080	0.092	0.084
$\sigma_{R_\sigma}^-$			0.079	0.071	0.082		0.088	0.093	0.085

$B_{\Lambda,i}^{\text{expt.}}$ and $\Delta B_{\Lambda,i}^{\text{expt.}}$ are taken from Ref. [126]. The eleven hypernuclei cover a large mass interval with $A = 12$ –208. When we made the fitting, it was found that the two ratios R_σ and R_ω both deviate from 2/3: The more light hypernuclei are included in the fitting, the smaller are the two ratios. This indicates that the in-medium ΛN couplings are suppressed by structure effects in light hypernuclei. To show such dependence of the deviations on the mass interval, we arrange

these eleven hypernuclei into three groups: (1) All of them ($A = 12$ –208), (2) nine of them ($^{16}_\Lambda\text{O}$ and heavier, i.e., $A = 16$ –208) and (3) only six of them ($^{40}_\Lambda\text{Ca}$ and heavier ones, i.e., $A = 40$ –208). Based on either of the two effective NN interactions DD-ME2 and PKDD, three new parameter sets are obtained. These six new effective interactions are labeled DD-ME2- Yi and PKDD- Yi with $i = 1, 2$, and 3 and are listed in Table I.

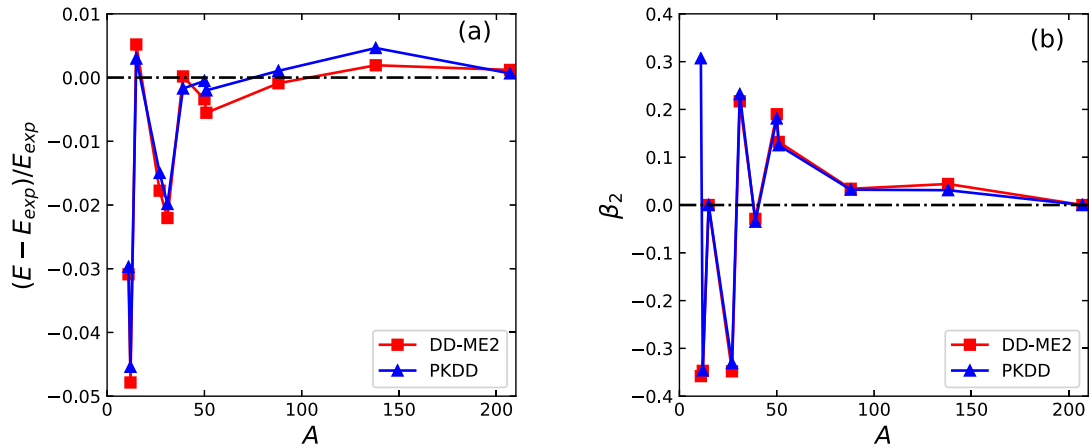


FIG. 1. (a) The relative deviations of the calculated binding energies of $^{11,12}_\Lambda\text{C}$, $^{15}_\Lambda\text{O}$, $^{27}_\Lambda\text{Si}$, $^{31}_\Lambda\text{S}$, $^{39}_\Lambda\text{Ca}$, $^{50,51}_\Lambda\text{V}$, $^{88}_\Lambda\text{Y}$, $^{138}_\Lambda\text{La}$, and $^{207}_\Lambda\text{Pb}$ from the experimental values [125] and (b) the quadrupole deformation parameters of these nuclei. The MDC-RMF calculations are carried out with density-dependent interactions DD-ME2 and PKDD, respectively.

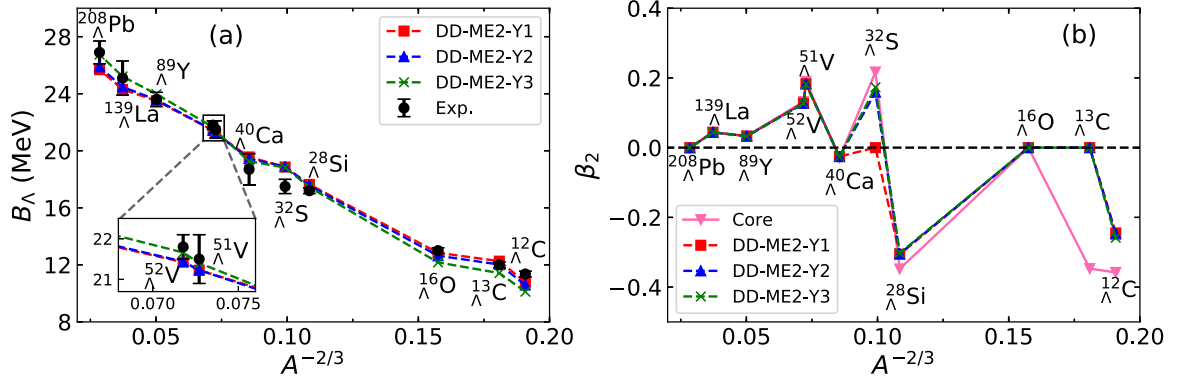


FIG. 2. (a) The calculated Λ separation energies compared with the experimental values and (b) the calculated quadrupole deformation parameters with DD-ME2-Y1, DD-ME2-Y2, and DD-ME2-Y3. The experimental values of B_Λ are taken from Ref. [7] except for $^{40}_{\Lambda}\text{Ca}$ [126]. The inset in panel (a) shows the results for $^{51,52}_{\Lambda}\text{V}$. The “Core” in panel (b) represents the quadrupole deformation parameters of the corresponding core nuclei calculated with DD-ME2.

From Table I, one can see that, if only six medium-heavy and heavy hypernuclei (those in Group 3) are used in the fitting, the average deviation $\bar{\chi}^2$ is the smallest which is around 0.2 for both DD-ME2-Y3 and PKDD-Y3. When more light hypernuclei are included, $\bar{\chi}^2$ becomes larger and the two ratios R_σ and R_ω become smaller. To check the overall description of the new effective interactions for all of these eleven hypernuclei, we calculate and list in Table I the average deviation $\bar{\chi}_{\text{all}}^2$ as defined in Eq. (8), the root mean square (rms) deviation Δ , and the root of relative square (rrs) deviation δ ,

$$\Delta = \sqrt{\frac{1}{N} \sum_i (B_{\Lambda,i}^{\text{expt.}} - B_{\Lambda,i}^{\text{calc.}})^2}, \quad (9)$$

$$\delta = \sqrt{\frac{1}{N} \sum_i \left(\frac{B_{\Lambda,i}^{\text{expt.}} - B_{\Lambda,i}^{\text{calc.}}}{B_{\Lambda,i}^{\text{expt.}}} \right)^2},$$

with $N = 11$, regardless of how many hypernuclei are used in the fitting. Therefore, $\bar{\chi}_{\text{all}}^2$ is larger than $\bar{\chi}^2$ for DD-ME2- Y_i and PKDD- Y_i with $i > 1$. For example, the average deviation $\bar{\chi}_{\text{all}}^2$ is 6.690 for DD-ME2-Y3 and 9.233 for PKDD-Y3. Such large $\bar{\chi}_{\text{all}}^2$ values are mainly due to the fact that the uncertainties of Λ separation energies of light hypernuclei are quite small, $\Delta B_{\Lambda,i}^{\text{expt.}} = 0.2$ MeV for $^{12,13}_{\Lambda}\text{C}$, $^{16}_{\Lambda}\text{O}$, and $^{28}_{\Lambda}\text{Si}$. Compared with $\bar{\chi}_{\text{all}}^2$, the rms and the rrs deviations are more adequate for describing the agreement between the calculation and experiment: $\Delta = 0.67\text{--}0.82$ MeV and $\delta = 3.8\%\text{--}5.4\%$ which are fairly small, meaning a reasonably good agreement.

The Λ separation energies B_Λ calculated with DD-ME2- Y_i ($i = 1, 2, \text{ and } 3$) are compared with experimental values in Fig. 2(a). It can be seen that each of these three new effective interactions can give a good description of B_Λ for the selected hypernuclei with an exception of $^{32}_{\Lambda}\text{S}$. Although all of these eleven hypernuclei are used in the parametrization fitting for DD-ME2-Y1, the light ones weigh more due to the smaller experimental errors $\Delta B_{\Lambda,i}^{\text{expt.}}$ (0.2 MeV). Therefore, with DD-ME2-Y1, the calculated separation energies of the four light hypernuclei are very close to the experimental values, while those of heavier hypernuclei deviate more from the experiment. With DD-ME2-Y3, the opposite is true: The calculated

B_Λ for heavy and medium-heavy hypernuclei, which are used in the fitting, are very close to the experiment while noticeable discrepancies can be seen for $^{12,13}_{\Lambda}\text{C}$, and $^{16}_{\Lambda}\text{O}$. As for $^{32}_{\Lambda}\text{S}$, the calculated B_Λ with these three parameter sets are very similar (18.865, 18.895, and 18.827 MeV) and all are considerably larger than the experimental value (17.5 ± 0.5 MeV). The reason for this discrepancy is not clear to us yet.

Figure 2(b) shows the quadrupole deformation parameters of the eleven selected hypernuclei calculated with DD-ME2- Y_i ($i = 1, 2, \text{ and } 3$) and of the corresponding core nuclei calculated with DD-ME2. From Fig. 2(b) one can find that the deformation parameter of a deformed hypernucleus is always smaller than that of its normal nuclear core. This is particularly true for light hypernuclei, e.g., $^{12}_{\Lambda}\text{C}$. Such shape polarization effects of Λ have been discussed in Refs. [75,77,127–131]. Although ^{12}C is obviously oblate with $\beta_2 = -0.347$, ^{13}C is spherical with DD-ME2- Y_i ($i = 1, 2, \text{ and } 3$); such a shape change is similar to that discussed in Ref. [75] where NL-RMF functionals were used. ^{32}S is spherical with DD-ME2-Y1, although its core, ^{31}S , is moderately deformed with $\beta_2 = 0.217$. DD-ME2-Y2 and DD-ME2-Y3 both predict a prolate $^{32}_{\Lambda}\text{S}$ with β_2 slightly smaller than that of ^{31}S . Similar discussions hold for Λ separation energies and deformation parameters calculated with PKDD- Y_i ($i = 1, 2, \text{ and } 3$) and will not be repeated.

Among the six parameter sets DD-ME2- Y_i and PKDD- Y_i ($i = 1, 2, \text{ and } 3$), the two ratios R_σ and R_ω change a lot. However, they are correlated linearly with each other, as shown in Fig. 3. We made a linear fit of these two parameters and the relation

$$R_\omega = 1.228R_\sigma - 0.097, \quad (10)$$

is obtained and shown as the blue line in Fig. 3. This linear relation can be explained as follows: In the RMF model, the central potentials U_B ($B = N$ or Λ) for Λ hypernuclei can be calculated from scalar and vector potentials approximately, $-U_B \approx g_{\sigma B}\sigma + g_{\omega B}\omega_0$. With the restriction $R_m = g_{m\Lambda}/g_{mN}$ ($m = \sigma$ or ω), one obtains

$$R_\omega \approx \frac{-U_\Lambda - R_\sigma g_{\sigma N}\sigma}{-U_N - g_{\sigma N}\sigma}. \quad (11)$$

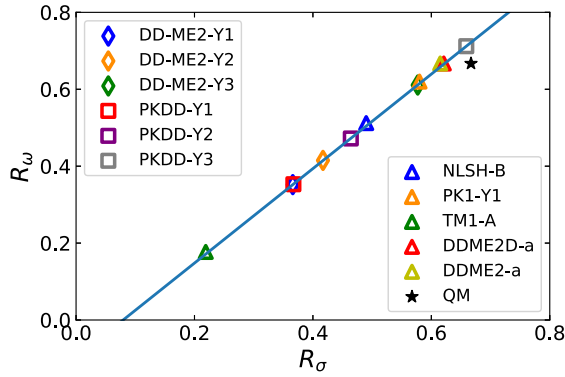


FIG. 3. The correlation between R_σ and R_ω in DD-ME2- Y_i and PKDD- Y_i ($i = 1, 2$, and 3). The blue line shows the linear relation (10) obtained by a linear fitting of R_σ and R_ω in these six parameter sets. Predictions from the quark model (QM), NL effective interactions NLSH-B [72], PK1-Y1 [121], and TM1-A [120] and DD effective interactions DDME2D-a [57] and DDME2-a [57] are also shown for comparison.

Generally speaking, the potential depths, represented by $U_B(0) \equiv U_B(r)|_{r=0}$, are about 70 MeV for nucleons and 30 MeV for Λ . The scalar potential depth $g_{\sigma N}\sigma(0)$ for nucleons is about -400 MeV. With these values, Eq. (11) becomes $R_\omega \approx 1.212R_\sigma - 0.091$, which is very close to Eq. (10). Similar linear behaviors between R_σ and R_ω in nonlinear parameter sets have been discussed in Refs. [51,121]. Several NL-RMF effective interactions NLSH-B [72], PK1-Y1 [121], and TM1-A [120] and DD-RMF effective interactions DDME2D-a [57] and DDME2-a [57] are also shown in Fig. 3. They all fall well on the line defined in Eq. (10). The ratios $R_\sigma = R_\omega = 2/3$ predicted from the quark model deviate from the blue line only slightly, as seen in Fig. 3. However, the Λ separation energies calculated with the corresponding parameter sets (DD-ME2-Y0 and PKDD-Y0) are much larger than the experimental values as listed in Table I. This means that these two ratios are connected strongly and correlate closely through the linear relation (10).

Next we analyze the errors of the parameters associated with the least-squares fitting by using the well-known strategy for error estimates from statistical analysis [132,133]. For each effective interaction, a physically reasonable parameter space is defined by a confidence region around R_σ and R_ω after normalization and the boundary of this space determines the errors of the parameters. Since the Λ separation energy is a highly nonlinear function of the parameters, the obtained confidence region is asymmetric with respect to R_σ and R_ω . Given a certain value of R_σ , the error of R_ω is quite small (less than 0.001) due to the strong correlation between the two ratios [cf. Eq. (10)]. Therefore, we only evaluate the errors $\sigma_{R_\sigma}^+$ and $\sigma_{R_\sigma}^-$ of the independent parameter R_σ for each effective interaction. As seen in Table I, $\sigma_{R_\sigma}^+$ and $\sigma_{R_\sigma}^-$ are smaller than 0.1 for all new effective interactions proposed in this work.

Λ separation energies in single- Λ excited states are not included in our fitting procedure. Next we calculate Λ separation energies in deformed single- Λ levels and average those from the same orbit with a fixed orbital angular momentum

l to obtain single- Λ separation energies in the p_Λ , d_Λ , f_Λ , and g_Λ orbits. In Fig. 4, results calculated with DD-ME2-Y2 and PKDD-Y2 are compared with experimental values taken from Refs. [7,126]. It can be seen that Λ separation energies in the p_Λ , d_Λ , f_Λ , and g_Λ single-particle states can be reproduced satisfactorily. For heavy hypernuclei ${}^{208}_\Lambda\text{Pb}$ and ${}^{139}_\Lambda\text{La}$, the theoretical Λ separation energies in the g_Λ state calculated with PKDD-Y2 match the experimental values well but those calculated with DD-ME2-Y2 are a little smaller than the experimental values. For light hypernucleus ${}^{12}_\Lambda\text{C}$, although it is weakly bound in the p_Λ state from both (π^+, K^+) and emulsion experiments, Λ is unbound from the new effective interactions DD-ME2-Y2 and PKDD-Y2.

These new effective interactions are obtained by adjustments to properties of hypernuclei. The question then arises as to how well the neutron-star properties can be described by them. The equations of state (EoSs) and mass-radius (M - R) relations of neutron stars are calculated with DD-ME2- Y_i ($i = 1, 2$, and 3) and shown in Fig. 5. The octet baryons p , n , Λ , Σ^\pm , Σ^0 , Ξ^0 , and Ξ^- and the leptons e^- and μ^- are considered. The vector coupling constants are determined by the naive quark model, i.e., $2g_{\omega\Sigma} = g_{\omega\Sigma} = 2g_{\omega N}/3$ for ωY coupling constants and $g_{\rho\Sigma} = 2g_{\rho\Sigma} = 2g_{\rho N}$ for ρY couplings. The scalar coupling constants $g_{\sigma\Sigma}$ and $g_{\sigma\Sigma}$ are constrained by the empirical potentials $U_\Sigma^{(N)} = 30$ MeV and $U_\Xi^{(N)} = -15$ MeV [134], respectively. The EoSs calculated with DD-ME2- Y_i ($i = 1, 2$, and 3) are the same as that with DD-ME2 at low energy density where only nucleons exist. When the energy density is larger than a certain value (about 300 MeV fm^{-3}), hyperons appear and the EoS is softer than that without hyperons, leading to the so-called ‘‘hyperon puzzle’’ [135,136]: Hyperons soften the EoS so that the maximum mass of neutron stars is smaller than $2M_\odot$, which is the lower limit of the maximum neutron-star mass as constrained from the astrophysical observations [137,138]. It can be seen in Fig. 5 that the larger the R_σ , the stiffer the EoS and the larger the maximum mass of neutron stars. With DD-ME2-Y1, DD-ME2-Y2, and DD-ME2-Y3, the maximum masses of neutron stars are, respectively, about $1.4M_\odot$, $1.5M_\odot$, and $1.8M_\odot$, which are all smaller than $2.5M_\odot$ with DD-ME2. The maximum mass calculated with the upper boundary of R_σ in DD-ME2-Y3 is $1.9M_\odot$ which is still smaller than $2M_\odot$. One way to stiffen the EoS and thus increase the maximum mass of hyperon stars is to introduce an additional repulsion from the exchange of ϕ mesons in the RMF framework [139]. A systematic study of ϕ -meson effects on the properties of hyperon stars in the DD-RMF model has been carried out, and it was found that the $2M_\odot$ limit for the maximum mass can be reached by using several relativistic density functionals with the ϕ meson included [140].

IV. SUMMARY

We investigate the effective interactions for Λ hypernuclei in the density-dependent relativistic mean-field model and propose new parameter sets. Based on effective NN interactions DD-ME2 and PKDD, the two ratios of scalar and vector coupling constants between effective ΛN and NN interactions, namely, R_σ and R_ω , are optimized by fitting calculated

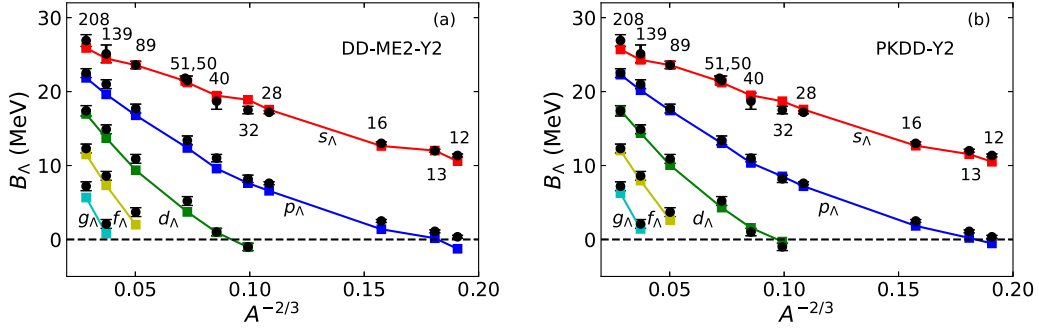


FIG. 4. The Λ separation energies in the s_Λ , p_Λ , d_Λ , f_Λ , and g_Λ single-particle states for ${}^A_\Lambda Z$ hypernuclei calculated with (a) DD-ME2-Y2 and (b) PKDD-Y2, respectively. The theoretical values are average separation energies of the deformed levels from s_Λ , p_Λ , d_Λ , f_Λ , and g_Λ single-particle states. The experimental values in black dots are taken from Refs. [7,126] and shown for comparison.

Λ separation energies to experimental values of eleven single- Λ hypernuclei with $A \geq 12$. The calculations were carried out by using the MDC-RMF model in which deformations are allowed for these hypernuclei and their normal core nuclei. With three ways of grouping and including these eleven selected Λ hypernuclei in the fitting, six new effective interactions DD-ME2-Y i and PKDD-Y i ($i = 1, 2$, and 3) are obtained. The two ratios R_σ and R_ω in these six new effective interactions vary largely, but they are correlated well with each other and follow closely a linear relation. The statistical error of the independent parameter R_σ is estimated and the error bars are within 0.1.

Ground-state properties of the eleven selected hypernuclei and the corresponding core nuclei are described well by the MDC-RMF model. For core nuclei, the calculated binding energies agree satisfactorily with the experiment and most of them are deformed. For hypernuclei, the calculated Λ separation energies are close to the experimental values with a small average square deviation weighed by experimental uncertainties. Shape polarization effects of Λ and the shape change of a hypernucleus compared with its core nucleus are obvious in the $A \leq 40$ mass region. Λ separation energies in single- Λ excited states are well reproduced although they are not used in

the fitting. The newly proposed effective interactions are also used to calculate the EoS of hypernuclear matter and study the mass and radius of neutron stars. It turns out that they fall into the “swamp,” which is full of effective interactions connected with the well-known “hyperon puzzle”: The lower limit of the maximum neutron-star mass, i.e., $2M_\odot$, cannot be reached because the EoS is not stiff enough when hyperons are considered.

ACKNOWLEDGMENTS

Helpful discussions with Johann Haidenbauer, Hoai Le, Andreas Nogga, Xiang-Xiang Sun, and Kun Wang are gratefully acknowledged. We thank Xiang-Xiang Sun for reading the paper and valuable suggestions. This work has been supported by the National Key R&D Program of China (Grant No. 2018YFA0404402), the National Natural Science Foundation of China (Grants No. 11525524, No. 12070131001, No. 12047503, and No. 11961141004), the Key Research Program of Frontier Sciences of Chinese Academy of Sciences (Grant No. QYZDB-SSWSYS013), and the Strategic Priority Research Program of Chinese Academy of Sciences (Grants No. XDB34010000 and No. XDPB15). The results

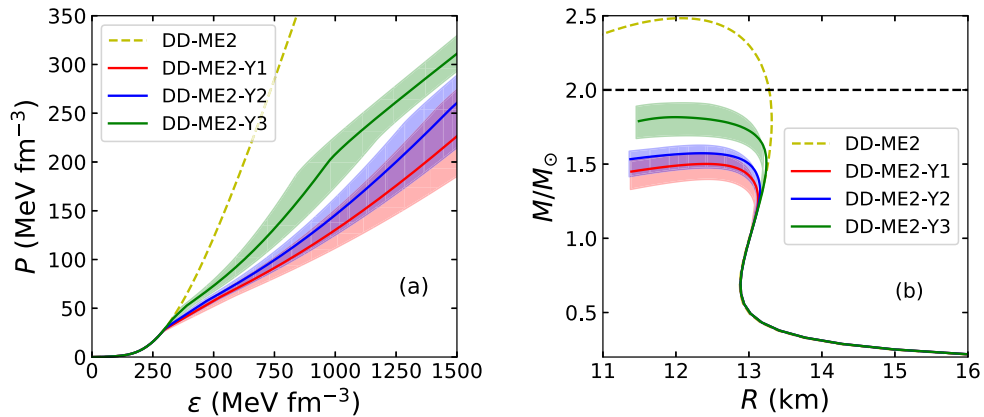


FIG. 5. (a) The equations of state and (b) the mass-radius relations for neutron stars with hyperons. The solid curves are calculated with DD-ME2-Y i ($i = 1, 2$, and 3) and the shaded areas are calculated with the corresponding upper and lower boundaries of R_σ in the correlated direction defined by Eq. (10). Results without hyperons (calculated with DD-ME2) are also shown for comparison.

described in this paper are obtained on the High-performance Computing Cluster of ITP-CAS and the ScGrid of the Super-

computing Center, Computer Network Information Center of Chinese Academy of Sciences.

-
- [1] E. Epelbaum, H.-W. Hammer, and Ulf-G. Meißner, *Rev. Mod. Phys.* **81**, 1773 (2009).
- [2] T. A. Rijken, M. M. Nagels, and Y. Yamamoto, *Prog. Theor. Phys. Suppl.* **185**, 14 (2010).
- [3] R. Machleidt and F. Sammarruca, *Phys. Scr.* **91**, 083007 (2016).
- [4] X.-L. Ren, K.-W. Li, L.-S. Geng, B. Long, P. Ring, and J. Meng, *Chin. Phys. C* **42**, 014103 (2018).
- [5] K.-W. Li, X.-L. Ren, L.-S. Geng, and B.-W. Long, *Chin. Phys. C* **42**, 014105 (2018).
- [6] T. A. Lähde and U.-G. Meißner, *Nuclear Lattice Effective Field Theory: An Introduction (Lecture Notes in Physics Book 957)* (Springer, New York, 2019).
- [7] A. Gal, E. V. Hungerford, and D. J. Millener, *Rev. Mod. Phys.* **88**, 035004 (2016).
- [8] L. Tolos and L. Fabbietti, *Prog. Part. Nucl. Phys.* **112**, 103770 (2020).
- [9] H. Tamura, S. Ajimura, H. Akikawa, D. Alburger, K. Aoki, A. Banu, R. Chrien, G. Franklin, J. Franz, Y. Fujii, Y. Fukao, T. Fukuda, O. Hashimoto, T. Hayakawa, E. Hiyama, H. Hotchi, K. Imai, W. Imoto, Y. Kakiguchi, M. Kameoka *et al.*, *Nucl. Phys. A* **754**, 58 (2005).
- [10] O. Hashimoto and H. Tamura, *Prog. Part. Nucl. Phys.* **57**, 564 (2006).
- [11] H. Tamura, *Prog. Theor. Exp. Phys.* **2012**, 02B012 (2012).
- [12] A. Esser, S. Nagao, F. Schulz, S. Bleser, M. Steinen, P. Achenbach, C. Ayerbe Gayoso, R. Böhm, O. Borodina, D. Bosnar, A. Botvina, V. Bozkurt, L. Debenjak, M. Distler, I. Friščić, Y. Fujii, T. Gogami, M. Gómez Rodríguez, O. Hashimoto, S. Hirose *et al.*, *Nucl. Phys. A* **914**, 519 (2013).
- [13] Y.-G. Ma, *J. Phys.: Conf. Ser.* **420**, 012036 (2013).
- [14] A. Feliciello and T. Nagae, *Rep. Prog. Phys.* **78**, 096301 (2015).
- [15] H. Takahashi, J. K. Ahn, H. Akikawa, S. Aoki, K. Arai, S. Y. Bahk, K. M. Baik, B. Bassalleck, J. H. Chung, M. S. Chung, D. H. Davis, T. Fukuda, K. Hoshino, A. Ichikawa, M. Ieiri, K. Imai, Y. H. Iwata, Y. S. Iwata, H. Kanda, M. Kaneko *et al.*, *Phys. Rev. Lett.* **87**, 212502 (2001).
- [16] K. Nakazawa, Y. Endo, S. Fukunaga, K. Hoshino, S. H. Hwang, K. Imai, H. Ito, K. Itonaga, T. Kanda, M. Kawasaki, J. H. Kim, S. Kinbara, H. Kobayashi, A. Mishina, S. Ogawa, H. Shibuya, T. Sugimura, M. K. Soe, H. Takahashi, T. Takahashi *et al.*, *Prog. Theor. Exp. Phys.* **2015**, 033D02 (2015).
- [17] S. H. Hayakawa *et al.* (J-PARC E07 Collaboration), *Phys. Rev. Lett.* **126**, 062501 (2021).
- [18] J. Adam *et al.* (STAR Collaboration), *Nat. Phys.* **16**, 409 (2020).
- [19] S. Beane, W. Detmold, K. Orginos, and M. Savage, *Prog. Part. Nucl. Phys.* **66**, 1 (2011).
- [20] S. R. Beane, E. Chang, S. D. Cohen, W. Detmold, P. Junnarkar, H. W. Lin, T. C. Luu, K. Orginos, A. Parreño, M. J. Savage, A. Walker-Loud *et al.* (NPLQCD Collaboration), *Phys. Rev. C* **88**, 024003 (2013).
- [21] S. Aoki *et al.* (HAL QCD Collaboration), *Prog. Theor. Exp. Phys.* **2012**, 01A105 (2012).
- [22] K. Sasaki *et al.* (HAL QCD Collaboration), *Prog. Theor. Exp. Phys.* **2015**, 113B01 (2015).
- [23] H. Polinder, J. Haidenbauer, and U.-G. Meißner, *Nucl. Phys. A* **779**, 244 (2006).
- [24] J. Haidenbauer and I. Vidaña, *Eur. Phys. J. A* **56**, 55 (2020).
- [25] X.-L. Ren, E. Epelbaum, and J. Gegelia, *Phys. Rev. C* **101**, 034001 (2020).
- [26] T. A. Rijken, V. G. J. Stoks, and Y. Yamamoto, *Phys. Rev. C* **59**, 21 (1999).
- [27] M. M. Nagels, T. A. Rijken, and Y. Yamamoto, *Phys. Rev. C* **99**, 044003 (2019).
- [28] B. Holzenkamp, K. Holinde, and J. Speth, *Nucl. Phys. A* **500**, 485 (1989).
- [29] A. Reuber, K. Holinde, H.-C. Kim, and J. Speth, *Nucl. Phys. A* **608**, 243 (1996).
- [30] J. Haidenbauer and Ulf-G. Meißner, *Phys. Rev. C* **72**, 044005 (2005).
- [31] D. E. Lanskoy, *Phys. Rev. C* **58**, 3351 (1998).
- [32] N. Guleria, S. K. Dhiman, and R. Shyam, *Nucl. Phys. A* **886**, 71 (2012).
- [33] H.-J. Schulze and E. Hiyama, *Phys. Rev. C* **90**, 047301 (2014).
- [34] J. Schaffner, C. Dover, A. Gal, C. Greiner, D. Millener, and H. Stocker, *Ann. Phys. (NY)* **235**, 35 (1994).
- [35] J. Mareš and B. K. Jennings, *Phys. Rev. C* **49**, 2472 (1994).
- [36] H. Shen, F. Yang, and H. Toki, *Prog. Theor. Phys.* **115**, 325 (2006).
- [37] Y.-T. Rong, P. Zhao, and S.-G. Zhou, *Phys. Lett. B* **807**, 135533 (2020).
- [38] J. D. Walecka, *Ann. Phys. (NY)* **83**, 491 (1974).
- [39] J. Boguta and A. Bodmer, *Nucl. Phys. A* **292**, 413 (1977).
- [40] B. D. Serot, *Phys. Lett. B* **86**, 146 (1979).
- [41] P.-G. Reinhard, *Z. Phys. A* **329**, 257 (1988).
- [42] Y. Sugahara and H. Toki, *Nucl. Phys. A* **579**, 557 (1994).
- [43] W. Long, J. Meng, N. Van Giai, and S. G. Zhou, *Phys. Rev. C* **69**, 034319 (2004).
- [44] R. Brockmann and H. Toki, *Phys. Rev. Lett.* **68**, 3408 (1992).
- [45] S. Haddad and M. K. Weigel, *Phys. Rev. C* **48**, 2740 (1993).
- [46] H. F. Boersma and R. Malfliet, *Phys. Rev. C* **49**, 233 (1994).
- [47] C. Fuchs, H. Lenske, and H. H. Wolter, *Phys. Rev. C* **52**, 3043 (1995).
- [48] H. Lenske and C. Fuchs, *Phys. Lett. B* **345**, 355 (1995).
- [49] S. Typel and H. H. Wolter, *Nucl. Phys. A* **656**, 331 (1999).
- [50] T. Nikšić, D. Vretenar, P. Finelli, and P. Ring, *Phys. Rev. C* **66**, 024306 (2002).
- [51] C. M. Keil, F. Hoffmann, and H. Lenske, *Phys. Rev. C* **61**, 064309 (2000).
- [52] F. Hofmann, C. M. Keil, and H. Lenske, *Phys. Rev. C* **64**, 025804 (2001).
- [53] P. Finelli, N. Kaiser, D. Vretenar, and W. Weise, *Nucl. Phys. A* **831**, 163 (2009).
- [54] G. Colucci and A. Sedrakian, *Phys. Rev. C* **87**, 055806 (2013).
- [55] S. Banik, M. Hempel, and D. Bandyopadhyay, *Astrophys. J., Suppl. Ser.* **214**, 22 (2014).
- [56] E. van Dalen, G. Colucci, and A. Sedrakian, *Phys. Lett. B* **734**, 383 (2014).

- [57] M. Fortin, S. S. Avancini, C. Providência, and I. Vidaña, *Phys. Rev. C* **95**, 065803 (2017).
- [58] C. Providência, M. Fortin, H. Pais, and A. Rabhi, *Front. Astron. Space Sci.* **6**, 13 (2019).
- [59] B. D. Serot and J. D. Walecka, *The Relativistic Nuclear Many-Body Problem*, Vol. 16 of Advances in Nuclear Physics, edited by J. W. Negele and E. Vogt (Plenum Press, New York, 1986).
- [60] P. G. Reinhard, *Rep. Prog. Phys.* **52**, 439 (1989).
- [61] P. Ring, *Prog. Part. Nucl. Phys.* **37**, 193 (1996).
- [62] M. Bender, P.-H. Heenen, and P.-G. Reinhard, *Rev. Mod. Phys.* **75**, 121 (2003).
- [63] D. Vretenar, A. Afanasjev, G. Lalazissis, and P. Ring, *Phys. Rep.* **409**, 101 (2005).
- [64] J. Meng, H. Toki, S. G. Zhou, S. Q. Zhang, W. H. Long, and L. S. Geng, *Prog. Part. Nucl. Phys.* **57**, 470 (2006).
- [65] T. Nikšić, D. Vretenar, and P. Ring, *Prog. Part. Nucl. Phys.* **66**, 519 (2011).
- [66] H. Liang, J. Meng, and S.-G. Zhou, *Phys. Rep.* **570**, 1 (2015).
- [67] J. Meng and S.-G. Zhou, *J. Phys. G* **42**, 093101 (2015).
- [68] S.-G. Zhou, *Phys. Scr.* **91**, 063008 (2016).
- [69] *Relativistic Density Functional for Nuclear Structure*, Vol. 10 of International Review of Nuclear Physics edition, edited by J. Meng (World Scientific Pub. Co. Pte. Ltd., 2016).
- [70] M. Rufa, J. Schaffner, J. Maruhn, H. Stöcker, W. Greiner, and P.-G. Reinhard, *Phys. Rev. C* **42**, 2469 (1990).
- [71] N. K. Glendenning and S. A. Moszkowski, *Phys. Rev. Lett.* **67**, 2414 (1991).
- [72] Z. Y. Ma, J. Speth, S. Krewald, B. Q. Chen, and A. Reuber, *Nucl. Phys. A* **608**, 305 (1996).
- [73] D. Vretenar, W. Pöschl, G. A. Lalazissis, and P. Ring, *Phys. Rev. C* **57**, R1060 (1998).
- [74] Y. N. Wang and H. Shen, *Phys. Rev. C* **81**, 025801 (2010).
- [75] B.-N. Lu, E.-G. Zhao, and S.-G. Zhou, *Phys. Rev. C* **84**, 014328 (2011).
- [76] Y. Tanimura and K. Hagino, *Phys. Rev. C* **85**, 014306 (2012).
- [77] B.-N. Lu, E. Hiyama, H. Sagawa, and S.-G. Zhou, *Phys. Rev. C* **89**, 044307 (2014).
- [78] S.-H. Ren, T.-T. Sun, and W. Zhang, *Phys. Rev. C* **95**, 054318 (2017).
- [79] T.-T. Sun, W.-L. Lu, and S.-S. Zhang, *Phys. Rev. C* **96**, 044312 (2017).
- [80] C. Horowitz and B. D. Serot, *Nucl. Phys. A* **368**, 503 (1981).
- [81] C. E. Price and G. E. Walker, *Phys. Rev. C* **36**, 354 (1987).
- [82] W. Pöschl, D. Vretenar, A. Rummel, and P. Ring, *Comput. Phys. Commun.* **101**, 75 (1997).
- [83] W. Pöschl, D. Vretenar, and P. Ring, *Comput. Phys. Commun.* **103**, 217 (1997).
- [84] Y. Gambhir, P. Ring, and A. Thimet, *Ann. Phys. (NY)* **198**, 132 (1990).
- [85] M. V. Stoitsov, W. Nazarewicz, and S. Pittel, *Phys. Rev. C* **58**, 2092 (1998).
- [86] L.-S. Geng, J. Meng, and H. Toki, *Chin. Phys. Lett.* **24**, 1865 (2007).
- [87] S.-G. Zhou, J. Meng, and P. Ring, *Phys. Rev. C* **68**, 034323 (2003).
- [88] S. Typel, *Front. Phys.* **6**, 73 (2018).
- [89] Z. X. Ren, S. Q. Zhang, and J. Meng, *Phys. Rev. C* **95**, 024313 (2017).
- [90] Z. X. Ren, S. Q. Zhang, Z. P. W., N. Itagaki, J. A. Maruhn, and J. Meng, *Sci. China: Phys., Mech. Astron.* **62**, 112062 (2019).
- [91] B.-N. Lu, E.-G. Zhao, and S.-G. Zhou, *Phys. Rev. C* **85**, 011301(R) (2012).
- [92] B.-N. Lu, J. Zhao, E.-G. Zhao, and S.-G. Zhou, *Phys. Rev. C* **89**, 014323 (2014).
- [93] B.-N. Lu, J. Zhao, E.-G. Zhao, and S.-G. Zhou, *Phys. Scr.* **89**, 054028 (2014).
- [94] J. Zhao, B.-N. Lu, D. Vretenar, E.-G. Zhao, and S.-G. Zhou, *Phys. Rev. C* **91**, 014321 (2015).
- [95] X. Meng, B. N. Lu, and S. G. Zhou, *Sci. China: Phys., Mech. Astron.* **63**, 212011 (2020).
- [96] J. Zhao, B.-N. Lu, E.-G. Zhao, and S.-G. Zhou, *Phys. Rev. C* **86**, 057304 (2012).
- [97] J. Zhao, B.-N. Lu, E.-G. Zhao, and S.-G. Zhou, *Phys. Rev. C* **95**, 014320 (2017).
- [98] C. Liu, S. Y. Wang, R. A. Bark, S. Q. Zhang, J. Meng, B. Qi, P. Jones, S. M. Wyngaardt, J. Zhao, C. Xu, S.-G. Zhou, S. Wang, D. P. Sun, L. Liu, Z. Q. Li, N. B. Zhang, H. Jia, X. Q. Li, H. Hua, Q. B. Chen *et al.*, *Phys. Rev. Lett.* **116**, 112501 (2016).
- [99] X. C. Chen, J. Zhao, C. Xu, H. Hua, T. M. Shneidman, S. G. Zhou, X. G. Wu, X. Q. Li, S. Q. Zhang, Z. H. Li, W. Y. Liang, J. Meng, F. R. Xu, B. Qi, Y. L. Ye, D. X. Jiang, Y. Y. Cheng, C. He, J. J. Sun, R. Han *et al.*, *Phys. Rev. C* **94**, 021301(R) (2016).
- [100] S. Perez-Martin and L. M. Robledo, *Phys. Rev. C* **78**, 014304 (2008).
- [101] G. A. Lalazissis, T. Nikšić, D. Vretenar, and P. Ring, *Phys. Rev. C* **71**, 024312 (2005).
- [102] S. Typel, *Phys. Rev. C* **71**, 064301 (2005).
- [103] W.-H. Long, N. Van Giai, and J. Meng, *Phys. Lett. B* **640**, 150 (2006).
- [104] W. Long, H. Sagawa, J. Meng, and N. V. Giai, *Europhys. Lett.* **82**, 12001 (2008).
- [105] W.-H. Long, H. Sagawa, N. V. Giai, and J. Meng, *Phys. Rev. C* **76**, 034314 (2007).
- [106] S. Typel, G. Röpke, T. Klähn, D. Blaschke, and H. H. Wolter, *Phys. Rev. C* **81**, 015803 (2010).
- [107] X. Roca-Maza, X. Viñas, M. Centelles, P. Ring, and P. Schuck, *Phys. Rev. C* **84**, 054309 (2011).
- [108] A. Taninah, S. Agbemava, A. Afanasjev, and P. Ring, *Phys. Lett. B* **800**, 135065 (2020).
- [109] B. Wei, Q. Zhao, Z.-H. Wang, J. Geng, B.-Y. Sun, Y.-F. Niu, and W.-H. Long, *Chin. Phys. C* **44**, 074107 (2020).
- [110] S. Typel and D. Alvear Terrero, *Eur. Phys. J. A* **56**, 160 (2020).
- [111] A. Bouyssy and J. Hüfner, *Phys. Lett. B* **64**, 276 (1976).
- [112] D. J. Millener, C. B. Dover, and A. Gal, *Phys. Rev. C* **38**, 2700 (1988).
- [113] S. Ajimura, H. Hayakawa, T. Kishimoto, H. Kohri, K. Matsuoka, S. Minami, T. Mori, K. Morikubo, E. Saji, A. Sakaguchi, Y. Shimizu, M. Sumihama, R. E. Chrien, M. May, P. Pile, A. Rusek, R. Sutter, P. Eugenio, G. Franklin, P. Khaustov *et al.*, *Phys. Rev. Lett.* **86**, 4255 (2001).
- [114] H. Akikawa, S. Ajimura, R. E. Chrien, P. M. Eugenio, G. B. Franklin, J. Franz, L. Gang, K. Imai, P. Khaustov, M. May, P. H. Pile, B. Quinn, A. Rusek, J. Sasao, R. I. Sawafta, H. Schmitt, H. Tamura, L. Tang, K. Tanida, L. Yuan *et al.*, *Phys. Rev. Lett.* **88**, 082501 (2002).
- [115] H. Kohri, S. Ajimura, H. Hayakawa, T. Kishimoto, K. Matsuoka, S. Minami, Y. S. Miyake, T. Mori, K. Morikubo, E. Saji, A. Sakaguchi, Y. Shimizu, M. Sumihama, R. E. Chrien, M. May, P. Pile, A. Rusek, R. Sutter, P. M. Eugenio, G. Franklin *et al.*, *Phys. Rev. C* **65**, 034607 (2002).

- [116] R. Brockmann and W. Weise, *Phys. Lett. B* **69**, 167 (1977).
- [117] H. J. Pirner, *Phys. Lett. B* **85**, 190 (1979).
- [118] J. V. Noble, *Phys. Lett. B* **89**, 325 (1980).
- [119] B. K. Jennings, *Phys. Lett. B* **246**, 325 (1990).
- [120] Y. Sugahara and H. Toki, *Prog. Theor. Phys.* **92**, 803 (1994).
- [121] X.-S. Wang, H.-Y. Sang, J.-H. Wang, and H.-F. Lü, *Commun. Theor. Phys.* **60**, 479 (2013).
- [122] J. Cohen and H. J. Weber, *Phys. Rev. C* **44**, 1181 (1991).
- [123] C. B. Dover and A. Gal, *Prog. Part. Nucl. Phys.* **12**, 171 (1984).
- [124] Y. Lim, C.-H. Lee, and Y. Oh, *Phys. Rev. D* **97**, 023010 (2018).
- [125] M. Wang, G. Audi, F. G. Kondev, W. J. Huang, S. Naimi, and X. Xu, *Chin. Phys. C* **41**, 030003 (2017).
- [126] P. H. Pile, S. Bart, R. E. Chrien, D. J. Millener, R. J. Sutter, N. Tsoupas, J.-C. Peng, C. S. Mishra, E. V. Hungerford, T. Kishimoto, L.-G. Tang, W. von Witsch, Z. Xu, K. Maeda, D. Gill, R. McCrady, B. Quinn, J. Seydoux, J. W. Sleight, R. L. Stearns *et al.*, *Phys. Rev. Lett.* **66**, 2585 (1991).
- [127] E. Hiyama, M. Kamimura, K. Miyazaki, and T. Motoba, *Phys. Rev. C* **59**, 2351 (1999).
- [128] X.-R. Zhou, H.-J. Schulze, H. Sagawa, C.-X. Wu, and E.-G. Zhao, *Phys. Rev. C* **76**, 034312 (2007).
- [129] M. T. Win and K. Hagino, *Phys. Rev. C* **78**, 054311 (2008).
- [130] M. T. Win, K. Hagino, and T. Koike, *Phys. Rev. C* **83**, 014301 (2011).
- [131] M. Isaka, M. Kimura, A. Dote, and A. Ohnishi, *Phys. Rev. C* **83**, 044323 (2011).
- [132] S. Brandt, *Data Analysis: Statistical and Computational Methods for Scientists and Engineers*, 4th ed. (Springer, New York, 2014).
- [133] J. Dobaczewski, W. Nazarewicz, and P.-G. Reinhard, *J. Phys. G* **41**, 074001 (2014).
- [134] C. Ishizuka, A. Ohnishi, K. Tsubakihara, K. Sumiyoshi, and S. Yamada, *J. Phys. G* **35**, 085201 (2008).
- [135] H.-J. Schulze, A. Polls, A. Ramos, and I. Vidaña, *Phys. Rev. C* **73**, 058801 (2006).
- [136] I. Vidaña, *Nucl. Phys. A* **914**, 367 (2013).
- [137] J. Antoniadis, P. C. C. Freire, N. Wex, T. M. Tauris, R. S. Lynch, M. H. van Kerkwijk, M. Kramer, C. Bassa, V. S. Dhillon, T. Driebe, J. W. T. Hessels, V. M. Kaspi, V. I. Kondratiev, N. Langer, T. R. Marsh, M. A. McLaughlin, T. T. Pennucci, S. M. Ransom, I. H. Stairs, J. van Leeuwen *et al.*, *Science* **340**, 1233232 (2013).
- [138] H. T. Cromartie, E. Fonseca, S. M. Ransom, P. B. Demorest, Z. Arzoumanian, H. Blumer, P. R. Brook, M. E. DeCesar, T. Dolch, J. A. Ellis, R. D. Ferdman, E. C. Ferrara, N. Garver-Daniels, P. A. Gentile, M. L. Jones, M. T. Lam, D. R. Lorimer, R. S. Lynch, M. A. McLaughlin, C. Ng *et al.*, *Nat. Astron.* **4**, 72 (2019).
- [139] I. Bednarek, P. Haensel, J. L. Zdunik, M. Bejger, and R. Mańka, *Astron. Astrophys.* **543**, A157 (2012).
- [140] Z.-H. Tu and S.-G. Zhou, [arXiv:2109.07678](https://arxiv.org/abs/2109.07678).